

# Intrasubspecific variations of the adult astragalar and calcaneal sizes in living Japanese raccoon dog (*Nyctereutes procyonoides viverrinus*)

現生ホンドタヌキの成獣における距骨および踵骨サイズの亜種内変異

Takehisa Tsubamoto

鶴本 武久

Earth's Evolution and Environment, Department of Mathematics, Physics, and Earth Sciences, Graduate School of Science and Engineering, Ehime University, 2-5 Bunkyo-cho, Matsuyama, Ehime Pref. 790-8577, Japan

愛媛大学 大学院理工学研究科 数理物質科学専攻 地球進化学講座

## Abstract.

The intrasubspecific variations of the adult astragalar and calcaneal sizes of living Japanese raccoon dog, *Nyctereutes procyonoides viverrinus* (Mammalia, Carnivora, Canidae), were examined to make basic data in considering the variations of fossil mammalian bones. The specimens consist of 63 adult individuals (35 males and 28 females). The data consist of 12 measurements for both the astragalus and calcaneum with a body mass and first and second molar sizes. There is no significant sexual dimorphism in all the measurements. The coefficients of variation (CV) of the astragalar and calcaneal sizes range from 3.7 to 5.9 and from 3.8 to 7.1, respectively, implying that the size variations of these two bones are relatively low. These CVs of the two bones are as low as those of the first and second molars (3.4–5.8). The correlation coefficient between the body mass and each astragalar and calcaneal measurement ranges from -0.05 to 0.47, implying that the correlation between the body mass and the astragalar and calcaneal sizes within *N. procyonoides viverrinus* is low or almost absent.

Key words: Key words: astragalus, basic statistics, calcaneum, calcaneus, Mammalia, Carnivora, talus

## Introduction

Tsubamoto (2019a) investigated intraspecific (intrasubspecific) variations of the astragalar and calcaneal sizes in living Japanese monkey, *Macaca fuscata fuscata* (Gray, 1870) (Mammalia, Primates, Cercopithecidae), to make basic data in considering the variations of fossil mammalian bones. Here, in addition, I investigate intrasubspecific variations of the adult astragalar and calcaneal sizes in living Japanese raccoon dog, *Nyctereutes procyonoides viverrinus* (Temminck, 1838) (Mammalia, Carnivora, Canidae). Although the cranioidal specimens of *N. procyonoides viverrinus* have been well investigated (Yamamoto, 1983; Yoshimura, 1983; Machida and Saito, 1986; Harada *et al.*, 1989, 1992; Kauhala *et al.*, 1998; Asahara, 2013, 2014a, 2014b; Tsubamoto, 2015; Asahara and Takai, 2017), its postcranial bones have been rarely studied. The sizes of the limb bones including the astragalus and calcaneum are usually more related to the body size of

animals than the sizes of the cranioidal specimens, so that the sizes and their variations of the limb bones are more useful for the paleoecological analyses using body size than those of the cranioidal specimens.

## Material and methods

All skeletal specimens of *N. procyonoides viverrinus* examined here are housed in Primate Research Institute, Kyoto University, Inuyama, Japan. The specimens consist of 63 adult individuals (35 males and 28 females) (Appendix Table A1). The specimens having erupted third molars and/or fused epiphyses of the long limb bones were identified as of adult individuals. The measurement positions of the astragalus and calcaneum (12 measurements for each bone) are indicated in Figure 1. For comparison, the body masses of the individuals were taken from the data base of the institute, and the length and width of the first and second molars of the individuals were also measured. The units of the linear

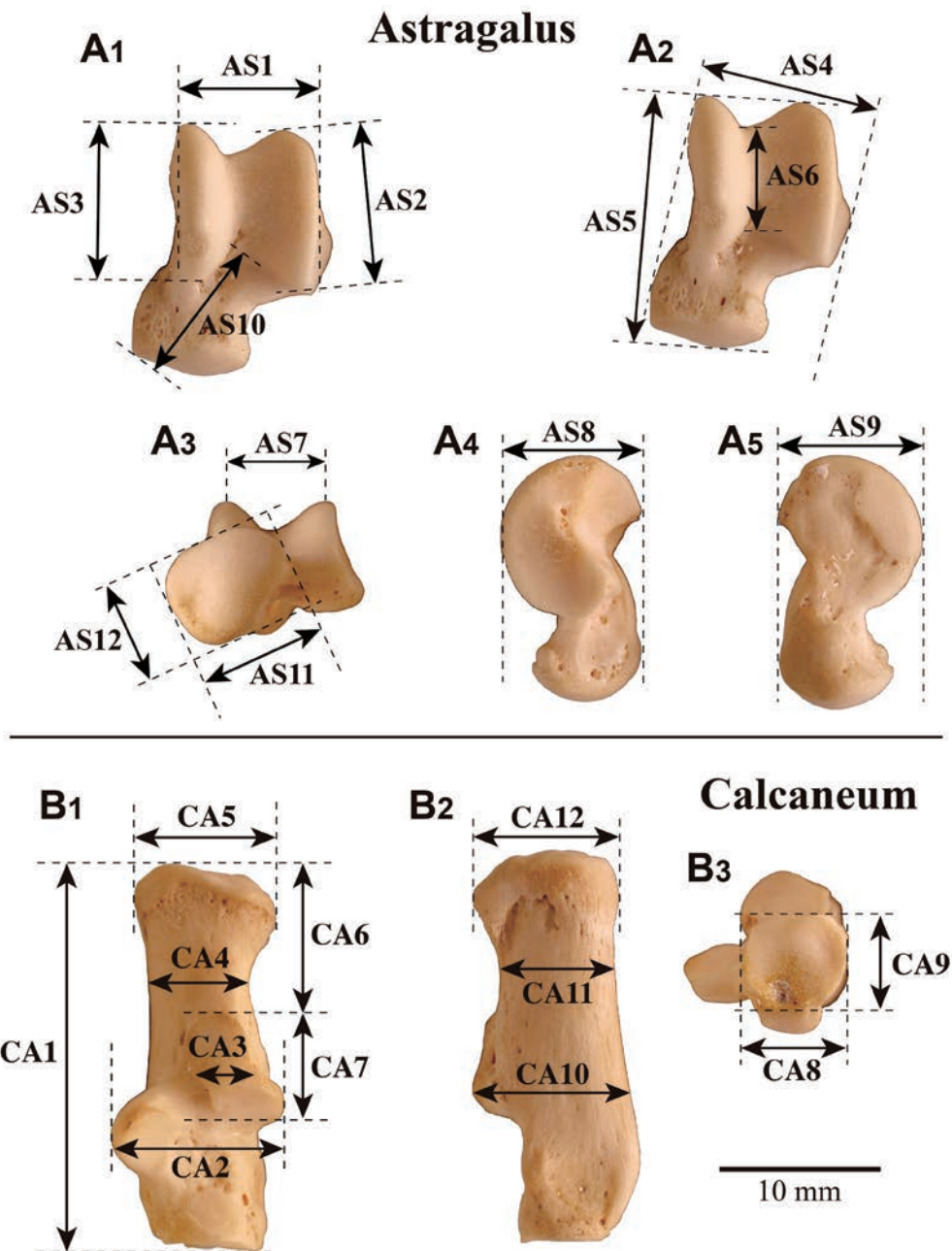


**Figure 1.** Measurement positions of the astragulus and calcaneum of *Nyctereutes procyonoides viverrinus* (Mammalia, Carnivora, Canidae) (after Tsubamoto, 2014, 2019a, 2019b; Tsubamoto et al., 2016). **A**, left astragulus: A<sub>1</sub>–A<sub>2</sub>, dorsal (anterior) view; A<sub>3</sub>, distal view; A<sub>4</sub>, lateral view; A<sub>5</sub>, medial view. *Linear measurements*.—AS1, medio-lateral width of the tibial trochlea; AS2, proximo-distal length of the lateral trochlear ridge of the tibial trochlea; AS3, proximo-distal length of the medial trochlear ridge of the tibial trochlea; AS4, medio-lateral width of the astragalus; AS5, proximo-distal length of the astragalus; AS6, proximo-distal length of the central part of the tibial trochlea; AS7, medio-lateral width between the medial and lateral trochlear ridges of the tibial trochlea; AS8, dorso-ventral thickness of the lateral part of the astragalus; AS9, dorso-ventral thickness of the medial part of the astragalus; AS10, neck-head length; AS11, width of the head; AS12, thickness of the head. **B**, left calcaneum: B<sub>1</sub>, dorsal (anterior) view; B<sub>2</sub>, lateral view; B<sub>3</sub>, distal view. *Linear measurements*.—CA1, calcaneal length; CA2, calcaneal width at the astragalar articular surfaces; CA3, width of the posterior astragalar articular surface; CA4, width of the posterior calcaneal body; CA5, width of the tuberosity; CA6, length of the posterior calcaneal body; CA7, length of the posterior astragalar articular surface; CA8, width of the articular surface for the cuboid; CA9, height of the articular surface for the cuboid; CA10, height at the posterior astragalar articular surface; CA11, height at the posterior calcaneal body; CA12, height at the tuberosity.

measurements and body mass are millimeter (mm) and gram (g), respectively. The linear measurements were taken to the nearest of 0.01 mm using digital calipers and were taken mostly on the left side when available. The analyses were carried out mostly using Excel (Microsoft) and JMP (SAS Institute Inc.), with VISUAL-SILVERMAN (Kusuhashi and Okamoto, 2015) for Silverman's test (Silverman, 1981, 1983).

*Abbreviations.*—AS1–AS12, measurement positions of the astragalus shown in Figure 1A; CA1–CA12, measurement positions of the calcaneum shown in Figure 1B; CV, coefficient of variation (unbiased); M1–M2/m1–m2, upper/lower first/second molars.

## Results and remarks

The basic statistics and distributions of all the measurements of the specimens are shown in Tables 1–4, Figures 2–5, and Appendix Figures A1–A2.

### Size distribution and sexual dimorphism

According to Welch's t test (5% significance level), there is no significant difference between males and females (sexual dimorphisms) in all measurements of the body mass, astragalus, calcaneum, and molars (Appendix Figures A1–A2). Each size distribution of the adult measurements including the body mass and M1–M2/m1–m2 is superficially unimodal generally (Figures 2–5). The tests of the normality for the linear measurements and log-normality for the body mass (5% significance level) were applied to the measurements. Most of the measurements could not reject the null hypothesis, but some measurements rejected it (Table 5). To test the multimodality of each adult measurement,

Silverman's test (5% significance level) (Silverman, 1981, 1983) was applied. All the measurements except the body mass could not reject the unimodal hypothesis, and the body mass rejected the unimodal hypothesis and could not reject the bimodal hypothesis. The distribution of the body mass can be identified as bimodal according to Silverman's test and also the histogram (Figure 2): the main peak at 3,000–3,250 g and the second peak at 4,500–4,750 g. This is not caused by the sexual dimorphism (Figure 2; Table 1). The reason for this bimodality is unclear.

### Coefficient of variation

To see and compare the degree of variation, CV is calculated. CVs of the astragalar and calcaneal sizes range from 3.7 to 5.9 and from 3.8 to 7.1, respectively (Tables 2–4), implying that the size variations of these two bones are relatively low and are lower than those of Japanese monkey (CVs: 6.5–9.1 and 6.9–10.8, respectively; Tsubamoto, 2019a). These CVs of the two bone sizes are as low as those of the first and second molar sizes (3.4–5.8). If we calculate CV separating the specimens into males and females, CVs of the adult astragalar and calcaneal sizes range as follows: astragulus (male), 3.9–6.1; astragulus (female), 3.4–6.2; calcaneum (male), 3.3–7.2; calcaneum (female), 3.8–7.5. These CVs of the two bones (separating males and females) are as low as those of the subspecies (uniting males and females).

**Table 1.** Basic statistics of the body mass (in gram). SD, standard deviation (unbiased); V, variance (unbiased); Max, maximum value; Min, minimum value; N, sample size; SE, standard error (unbiased).

	All	Male	Female
SD	573	580	564
V	328,530	335,849	317,855
Mean	3,719	3,651	3,805
Median	3,600	3,400	3,700
Max	5,100	5,100	5,000
Min	2,800	2,800	3,000
N	63	35	28
SE	72	98	107
Skewness	0.76	0.86	0.75
Kurtosis	-0.40	-0.10	-0.57

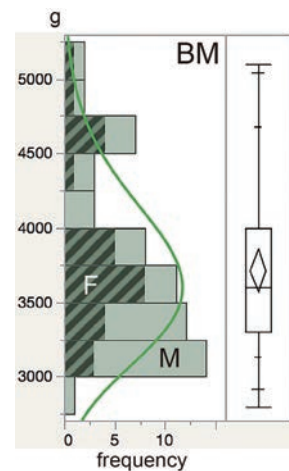


**Figure 2.** Histogram and box plot of the body mass (BM). The box plot shows quartiles with arithmetic mean (diamond) and whiskers from minimum to maximum with 2.5th, 10th, 90th, and 97.5th percentiles. Green line indicates the fitting for log-normal distribution. F, female; M, male.

**Table 2.** Basic statistics of the astragalar measurements (in mm). CV, coefficient of variation (unbiased); AS1–AS12, measurement points of the astragalus shown in Figure 1A. Other abbreviations are indicated in Table 1.

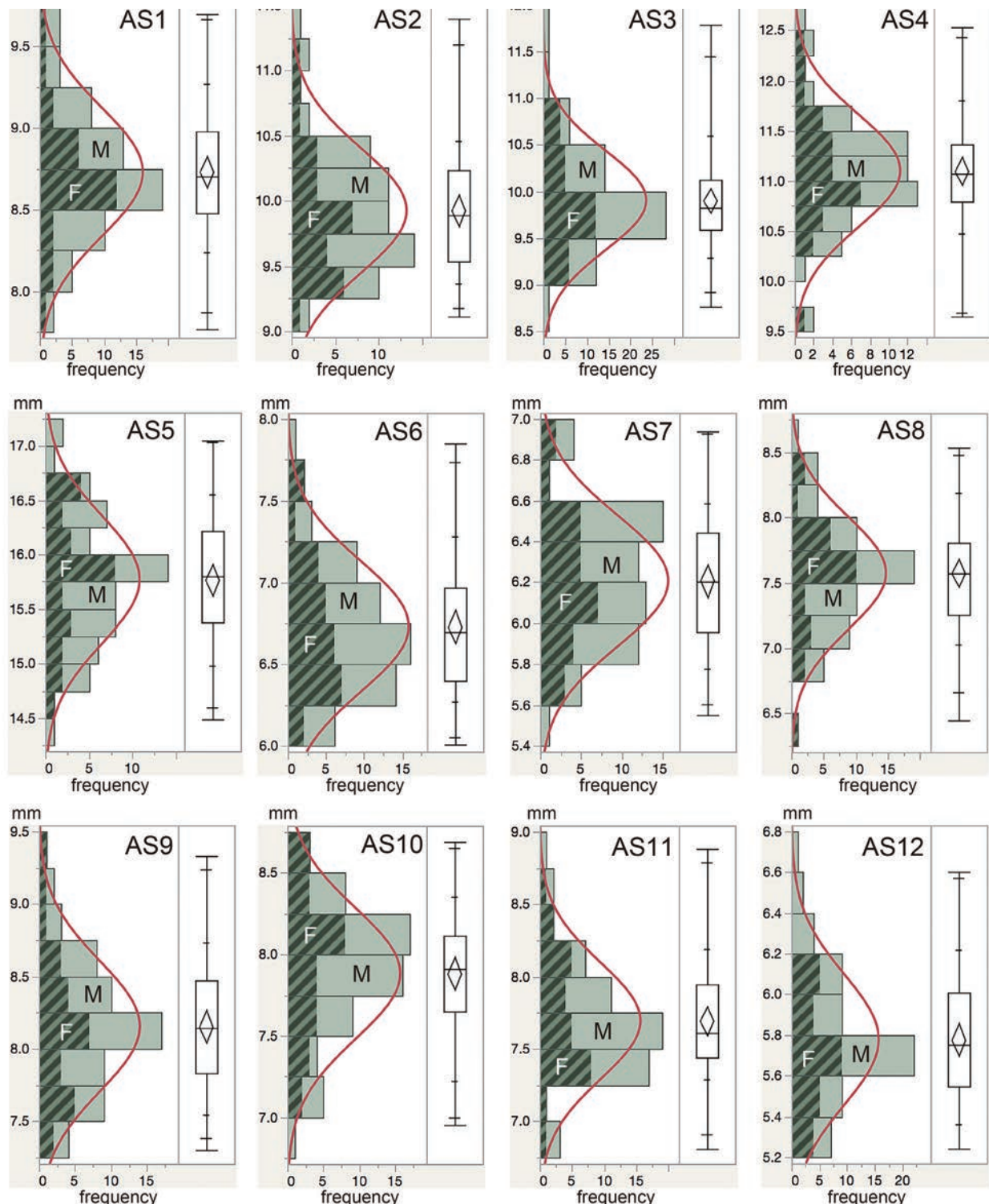
All	AS1	AS2	AS3	AS4	AS5	AS6	AS7	AS8	AS9	AS10	AS11	AS12
CV	4.49	4.80	5.37	5.04	3.69	5.90	5.14	5.64	5.49	5.08	5.22	5.54
SD	0.39	0.48	0.53	0.56	0.58	0.40	0.32	0.43	0.45	0.40	0.40	0.32
V	0.15	0.23	0.28	0.31	0.34	0.16	0.10	0.18	0.20	0.16	0.16	0.10
Mean	8.73	9.93	9.90	11.10	15.77	6.73	6.21	7.57	8.16	7.88	7.69	5.78
Median	8.70	9.89	9.82	11.07	15.80	6.70	6.20	7.57	8.14	7.91	7.61	5.75
Max	9.70	11.40	11.79	12.53	17.05	7.85	6.94	8.53	9.33	8.69	8.88	6.60
Min	7.77	9.11	8.76	9.65	14.49	6.01	5.55	6.45	7.3	6.95	6.81	5.24
N	63	63	63	63	63	63	63	63	63	63	63	63
SE	0.05	0.06	0.07	0.07	0.07	0.05	0.04	0.05	0.06	0.05	0.05	0.04
Skewness	0.19	0.81	0.89	0.12	0.04	0.62	0.22	0.06	0.37	-0.48	0.65	0.53
Kurtosis	0.14	0.72	1.86	0.90	-0.38	0.12	-0.34	0.09	-0.14	-0.05	0.80	0.09

Male	AS1	AS2	AS3	AS4	AS5	AS6	AS7	AS8	AS9	AS10	AS11	AS12
CV	4.84	4.91	5.82	5.06	3.94	5.79	5.27	5.82	4.96	4.74	5.18	6.11
SD	0.42	0.49	0.58	0.56	0.62	0.39	0.33	0.44	0.40	0.37	0.40	0.36
V	0.18	0.24	0.33	0.31	0.38	0.15	0.11	0.19	0.16	0.14	0.16	0.13
Mean	8.74	9.94	9.91	11.08	15.74	6.71	6.21	7.57	8.16	7.85	7.67	5.84
Median	8.73	9.92	9.81	11.08	15.71	6.62	6.24	7.57	8.16	7.89	7.61	5.76
Max	9.70	11.40	11.79	12.53	17.05	7.85	6.94	8.53	9.05	8.40	8.88	6.60
Min	7.94	9.11	8.76	9.65	14.49	6.01	5.55	6.81	7.45	6.95	6.81	5.24
N	35	35	35	35	35	35	35	35	35	35	35	35
SE	0.07	0.08	0.10	0.09	0.10	0.07	0.06	0.07	0.07	0.06	0.07	0.06
Skewness	0.34	0.89	1.11	0.23	0.28	0.72	0.06	0.53	0.26	-0.86	1.00	0.47
Kurtosis	-0.26	1.29	2.60	1.55	-0.26	0.84	-0.40	-0.21	-0.40	0.28	2.84	-0.38

Female	AS1	AS2	AS3	AS4	AS5	AS6	AS7	AS8	AS9	AS10	AS11	AS12
CV	4.09	4.74	4.85	5.10	3.40	6.11	5.08	5.52	6.19	5.51	5.33	4.45
SD	0.36	0.47	0.48	0.57	0.54	0.41	0.32	0.42	0.50	0.44	0.41	0.25
V	0.13	0.22	0.23	0.32	0.29	0.17	0.10	0.18	0.25	0.19	0.17	0.06
Mean	8.72	9.90	9.89	11.12	15.81	6.76	6.20	7.58	8.15	7.92	7.72	5.70
Median	8.70	9.86	9.86	11.04	15.82	6.72	6.16	7.67	8.11	7.99	7.62	5.72
Max	9.50	11.01	10.99	12.31	16.71	7.66	6.92	8.33	9.33	8.69	8.50	6.16
Min	7.77	9.23	9.02	9.71	14.68	6.08	5.64	6.45	7.30	7.03	6.98	5.24
N	28	28	28	28	28	28	28	28	28	28	28	28
SE	0.07	0.09	0.09	0.11	0.10	0.08	0.06	0.08	0.10	0.08	0.08	0.05
Skewness	-0.16	0.74	0.40	-0.02	-0.32	0.53	0.46	-0.64	0.47	-0.29	0.28	-0.07
Kurtosis	1.13	0.20	-0.03	0.56	-0.35	-0.38	-0.05	0.90	-0.05	-0.34	-0.92	-0.60



**Figure 3.** Histograms and box plots of the astragalar measurements. Red line indicates the fitting for the normal distribution. The explanations of the box plots are shown in Figure 2. Abbreviations are shown in Figures 1–2.

**Table 3.** Basic statistics of the calcaneal measurements (in mm). CA1–CA12, measurement points of the calcaneum shown in Figure 1B. Other abbreviations are indicated in Tables 1–2.

All	CA1	CA2	CA3	CA4	CA5	CA6	CA7	CA8	CA9	CA10	CA11	CA12
CV	3.78	4.39	6.57	6.73	5.44	6.69	5.12	5.70	7.11	3.85	5.01	6.27
SD	0.90	0.46	0.28	0.28	0.35	0.66	0.43	0.40	0.41	0.38	0.37	0.56
V	0.81	0.21	0.08	0.08	0.12	0.44	0.18	0.16	0.17	0.14	0.14	0.31
Mean	23.87	10.39	4.24	4.22	6.41	9.87	8.34	6.99	5.75	9.85	7.36	8.92
Median	23.90	10.41	4.22	4.19	6.35	9.90	8.34	6.98	5.74	9.84	7.38	8.97
Max	25.55	11.45	5.12	5.03	7.21	11.29	9.22	7.89	6.51	10.82	8.09	10.10
Min	20.85	9.07	3.58	3.80	5.72	7.59	7.44	6.11	4.88	9.07	6.43	7.35
N	63	63	63	63	63	63	63	63	63	63	63	63
SE	0.11	0.06	0.04	0.04	0.04	0.08	0.05	0.05	0.05	0.05	0.05	0.07
Skewness	-0.55	0.01	0.35	0.57	0.25	-0.53	-0.22	0.18	-0.28	0.41	-0.08	-0.46
Kurtosis	0.72	0.39	0.66	-0.07	-0.22	0.97	-0.55	-0.34	-0.70	0.27	-0.45	0.24
Male	CA1	CA2	CA3	CA4	CA5	CA6	CA7	CA8	CA9	CA10	CA11	CA12
CV	3.25	4.88	6.29	7.19	4.87	6.08	5.04	5.55	6.92	3.83	4.52	5.26
SD	0.78	0.51	0.27	0.30	0.31	0.60	0.42	0.39	0.39	0.38	0.33	0.48
V	0.60	0.26	0.07	0.09	0.10	0.36	0.17	0.15	0.16	0.14	0.11	0.23
Mean	23.94	10.38	4.28	4.23	6.45	9.93	8.31	6.96	5.70	9.90	7.36	9.04
Median	23.88	10.30	4.26	4.20	6.37	10.06	8.31	6.98	5.74	9.89	7.39	9.08
Max	25.55	11.45	5.12	5.03	7.21	11.29	9.04	7.82	6.51	10.82	7.95	10.10
Min	22.46	9.07	3.84	3.82	5.73	8.98	7.44	6.11	4.95	9.24	6.74	7.84
N	35	35	35	35	35	35	35	35	35	35	35	35
SE	0.13	0.09	0.05	0.05	0.05	0.10	0.07	0.07	0.07	0.06	0.06	0.08
Skewness	0.25	0.23	0.80	0.76	0.50	0.10	-0.25	0.14	-0.17	0.82	-0.10	-0.20
Kurtosis	-0.65	0.57	1.39	0.28	0.55	-0.60	-0.45	0.13	-0.48	0.75	-0.81	0.45
Female	CA1	CA2	CA3	CA4	CA5	CA6	CA7	CA8	CA9	CA10	CA11	CA12
CV	4.39	3.76	6.87	6.21	6.09	7.45	5.28	5.94	7.31	3.87	5.65	7.14
SD	1.04	0.39	0.29	0.26	0.39	0.73	0.44	0.42	0.43	0.38	0.42	0.63
V	1.09	0.15	0.08	0.07	0.15	0.53	0.20	0.17	0.18	0.14	0.17	0.39
Mean	23.77	10.39	4.20	4.21	6.35	9.80	8.38	7.02	5.81	9.80	7.35	8.77
Median	23.95	10.49	4.21	4.18	6.32	9.86	8.43	7.00	5.89	9.79	7.37	8.74
Max	25.42	10.88	4.79	4.65	7.07	10.85	9.22	7.89	6.44	10.54	8.09	9.72
Min	20.85	9.52	3.58	3.80	5.72	7.59	7.47	6.31	4.88	9.07	6.43	7.35
N	28	28	28	28	28	28	28	28	28	28	28	28
SE	0.20	0.07	0.05	0.05	0.07	0.14	0.08	0.08	0.08	0.07	0.08	0.12
Skewness	-0.86	-0.61	-0.02	0.17	0.24	-0.91	-0.22	0.20	-0.48	-0.07	-0.07	-0.34
Kurtosis	0.70	-0.74	-0.21	-1.03	-0.77	1.62	-0.56	-0.70	-0.68	-0.64	-0.36	-0.30

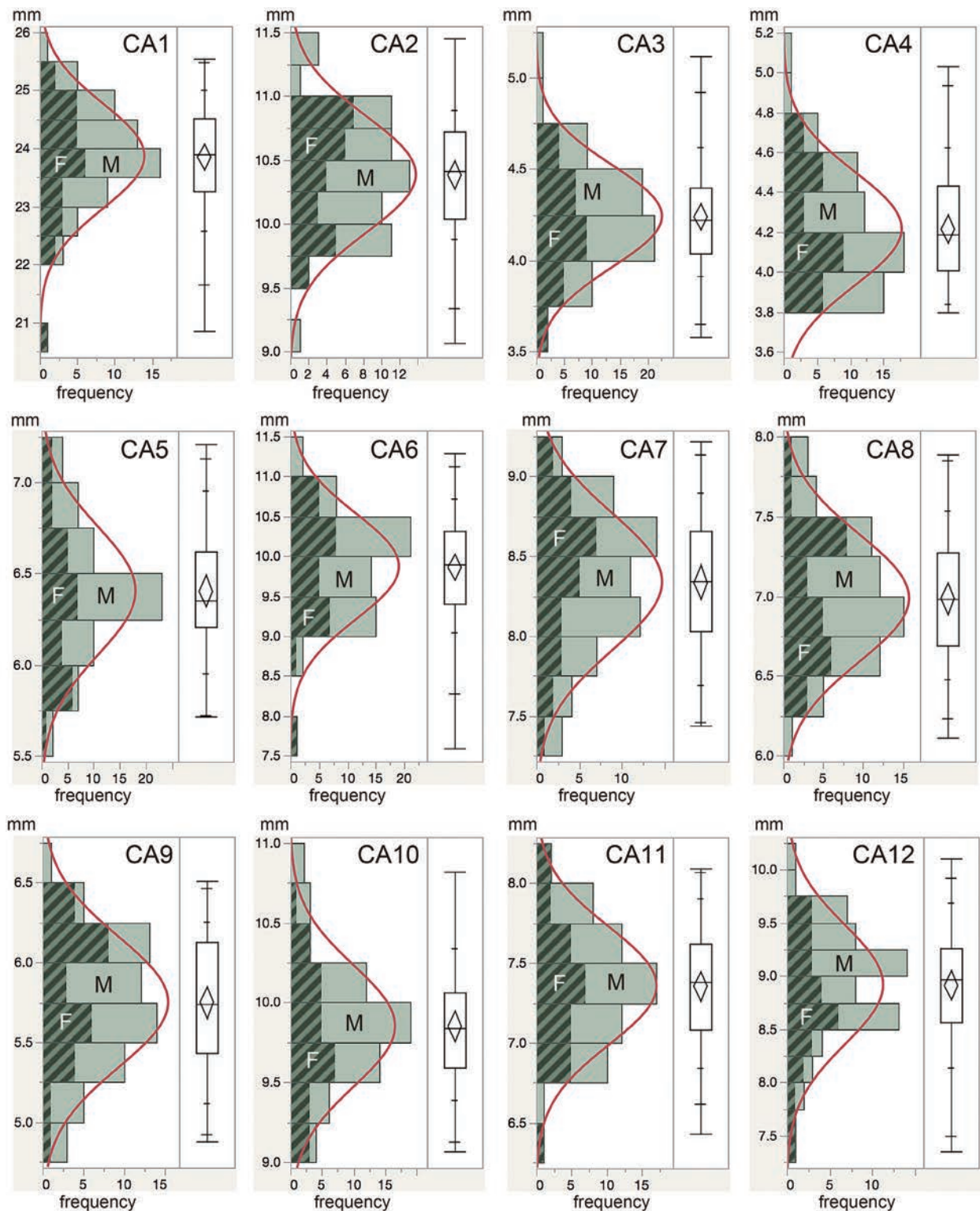


**Figure 4.** Histograms and box plots of the calcaneal measurements. The explanations of the box plots are shown in Figure 2. Abbreviations are shown in Figures 1–2.

**Table 4.** Basic statistics of the molar measurements (in mm). M1–M2/m1–m2, upper/lower molars; L, maximum length; W, maximum width. Other abbreviations are indicated in Tables 1–2.

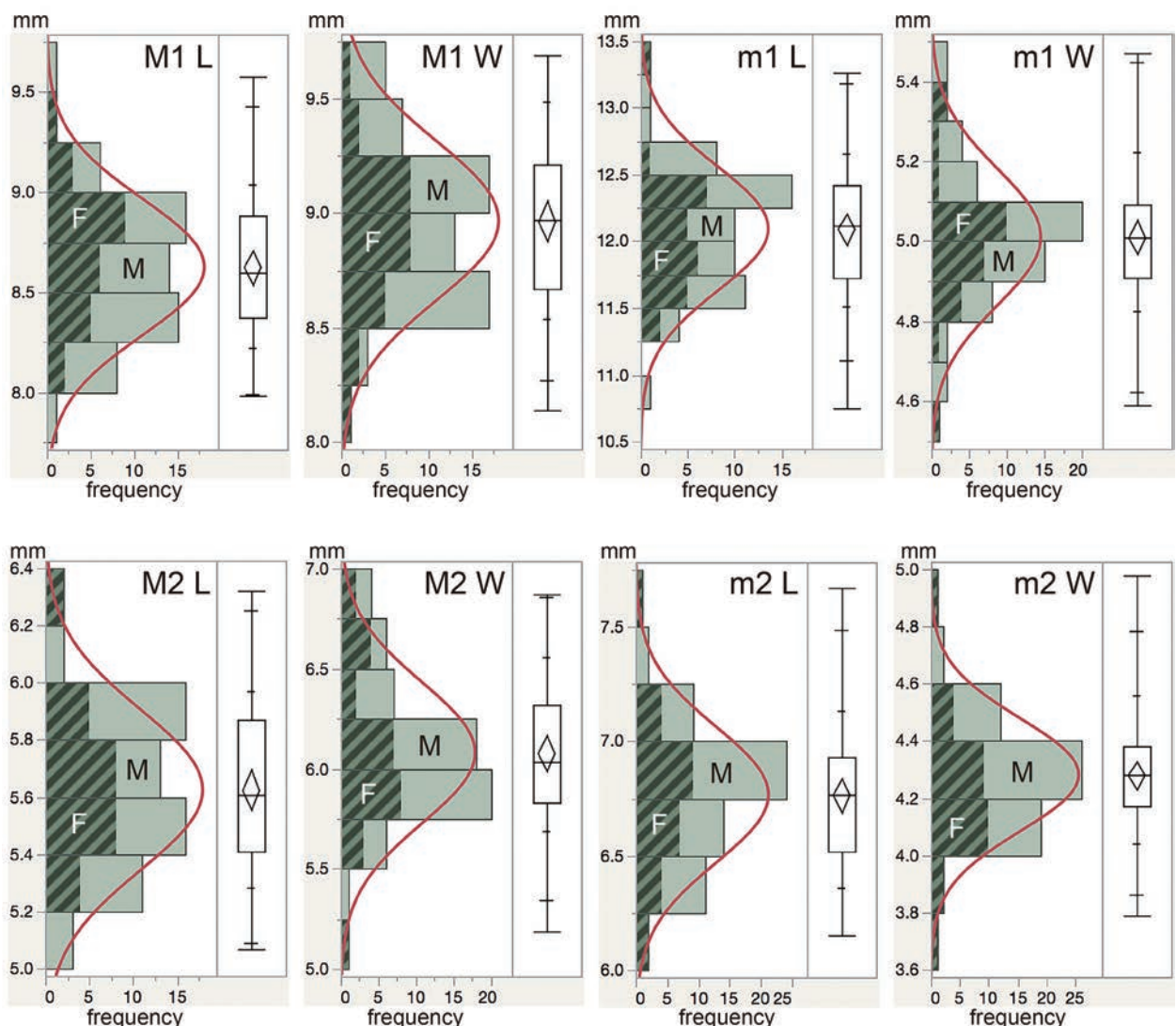
All	M1 L	M1 W	M2 L	M2 W	m1 L	m1 W	m2 L	m2 W
CV	3.95	3.87	4.98	5.79	3.83	3.39	4.38	4.59
SD	0.34	0.35	0.28	0.35	0.46	0.17	0.30	0.20
V	0.12	0.12	0.08	0.12	0.21	0.03	0.09	0.04
Mean	8.63	8.97	5.62	6.08	12.09	5.01	6.77	4.28
Median	8.60	8.97	5.61	6.03	12.12	5.01	6.77	4.28
Max	9.58	9.69	6.32	6.87	13.26	5.47	7.67	4.98
Min	7.98	8.14	5.07	5.19	10.75	4.59	6.15	3.79
N	62	63	63	63	63	62	63	63
SE	0.04	0.04	0.04	0.04	0.06	0.02	0.04	0.02
Skewness	0.31	0.06	0.16	0.30	-0.08	0.24	0.25	0.56
Kurtosis	-0.17	-0.49	-0.50	0.02	0.34	0.95	0.42	1.84

Male	M1 L	M1 W	M2 L	M2 W	m1 L	m1 W	m2 L	m2 W
CV	4.05	3.85	5.04	4.92	4.05	3.63	4.01	3.67
SD	0.35	0.35	0.28	0.30	0.49	0.18	0.27	0.16
V	0.12	0.12	0.08	0.09	0.24	0.03	0.07	0.02
Mean	8.56	8.98	5.59	6.04	12.14	5.02	6.78	4.31
Median	8.52	8.97	5.55	6.00	12.22	5.01	6.78	4.28
Max	9.58	9.69	6.12	6.78	13.14	5.47	7.36	4.65
Min	7.98	8.41	5.07	5.45	10.75	4.65	6.33	4.04
N	35	35	35	35	35	34	35	35
SE	0.06	0.06	0.05	0.05	0.08	0.03	0.05	0.03
Skewness	0.74	0.30	-0.04	0.36	-0.58	0.34	0.14	0.49
Kurtosis	0.77	-0.73	-1.01	-0.11	0.54	0.74	-0.43	-0.45

Female	M1 L	M1 W	M2 L	M2 W	m1 L	m1 W	m2 L	m2 W
CV	3.69	3.95	4.88	6.69	3.55	3.12	4.89	5.54
SD	0.32	0.35	0.28	0.41	0.43	0.16	0.33	0.24
V	0.10	0.12	0.08	0.17	0.18	0.02	0.11	0.06
Mean	8.71	8.95	5.67	6.13	12.04	5.00	6.75	4.25
Median	8.75	8.98	5.63	6.11	12.02	5.01	6.77	4.25
Max	9.32	9.55	6.32	6.87	13.26	5.36	7.67	4.98
Min	8.00	8.14	5.20	5.19	11.34	4.59	6.15	3.79
N	27	28	28	28	28	28	28	28
SE	0.06	0.07	0.05	0.08	0.08	0.03	0.06	0.04
Skewness	-0.20	-0.21	0.48	0.10	0.76	-0.04	0.38	0.81
Kurtosis	-0.40	-0.18	-0.07	-0.18	1.07	1.51	1.02	2.39



**Figure 5.** Histogram and box plot of the measurements of M1–M2/m1–m2. The explanations of the box plots are shown in Figure 2. L, maximum length; W, maximum width. Other abbreviations are shown in Figures 2–3.

#### Correlation with body mass

The correlation coefficients between the body mass and the astragalar and calcaneal measurements are generally higher than those between the body mass and the molar measurements (Table 6; Appendix Figure A3). The correlation coefficient between the body mass and each astragalar measurement ranges from 0.01 to 0.42; that between the body mass and each calcaneal measurement ranges from -0.05 to 0.47; and that between the body mass and each molar measurement ranges from -0.04 to 0.17 (Table 6). These results imply that the correlation between the body mass and the adult

astragalar and calcaneal sizes within the subspecies *N. procyonoides viverrinus* is low or almost absent.

#### Concluding remarks

Here, I investigated intrasubspecific variations of the various astragalar and calcaneal sizes in the adult specimens of living *N. procyonoides viverrinus*. The sizes of the two bones of this subspecies did not show any sexual dimorphism. The results will be additional basic data in interpreting the variations of mammalian astragali and calcanea discovered in paleontological and archaeozoological sites.

**Table 5.** Goodness-of-fit tests of the fittings for the normal and log-normal distributions. The normal test is for the linear measurements, and the log-normal test is for the body mass. The Shapiro-Wilk and Kolmogorov-Smirnov tests were used for the tests of normality and log-normality, respectively. \*,  $p$ -value < 0.05. Abbreviations are shown in Figures 1–2 and Tables 1–4.

	Normality ( $p$ -value)	Lognormality ( $p$ -value)
BM	—	0.0407*
AS1	0.9327	—
AS2	0.0110*	—
AS3	0.0318*	—
AS4	0.2639	—
AS5	0.9133	—
AS6	0.1112	—
AS7	0.6688	—
AS8	0.7443	—
AS9	0.4186	—
AS10	0.1071	—
AS11	0.0708	—
AS12	0.0813	—
CA1	0.2151	—
CA2	0.6173	—
CA3	0.7980	—
CA4	0.0551	—
CA5	0.2477	—
CA6	0.1174	—
CA7	0.5758	—
CA8	0.8976	—
CA9	0.2384	—
CA10	0.3825	—
CA11	0.7214	—
CA12	0.4109	—
M1 L	0.5828	—
M1 W	0.6853	—
M2 L	0.6674	—
M2 W	0.2900	—
m1 L	0.7718	—
m1 W	0.2047	—
m2 L	0.6815	—
m2 W	0.1342	—

**Table 6.** Pearson's correlation coefficient between the body mass and each measurement. Abbreviations are shown in Figure 1 and Tables 1–4.

AS1	0.20	M1 L	-0.03
AS2	0.25	M1 W	-0.04
AS3	0.29	M2 L	0.17
AS4	0.33	M2 W	0.03
AS5	0.23	m1 L	-0.04
AS6	0.34	m1 W	0.02
AS7	0.01	m2 L	0.01
AS8	0.01	m2 W	0.02
AS9	0.18		
AS10	0.12		
AS11	0.42		
AS12	0.37		
CA1	0.30		
CA2	0.17		
CA3	-0.05		
CA4	0.37		
CA5	0.25		
CA6	0.37		
CA7	0.47		
CA8	0.27		
CA9	0.41		
CA10	0.35		
CA11	0.23		
CA12	0.08		

### Acknowledgments

I am grateful to Masanaru Takai, Takeshi Nishimura, and Naoko Egi (Primate Research Institute, Kyoto University, Inuyama, Japan) for graciously providing access to the specimens examined. This manuscript was improved by the reviews of Masaya Matsuura and Nao Kusuhashi (Ehime University, Matsuyama, Japan). This research was partly supported by the Cooperation Program (2014-B-2) of Primate Research Institute (Kyoto University, Inuyama, Japan).

### References

- Asahara, M., 2013: Shape variation in the skull and lower carnassial in a wild population of raccoon dog (*Nyctereutes procyonoides*). *Zoological Science*, **30**: 205–210.

- Asahara, M., 2014a: Evolution of relative lower molar sizes among local populations of the raccoon dog (*Nyctereutes procyonoides*) in Japan. *Mammal Study*, **39**: 181–184.
- Asahara, M., 2014b: Shape variation in the skull within and between wild populations of the raccoon dog (*Nyctereutes procyonoides*) in Japan. *Mammal Study*, **39**: 105–113.
- Asahara, M. and Takai M., 2017: Estimation of diet in extinct raccoon dog species by the molar ratio method. *Acta Zoologica*, **98**: 292–299.
- Gray, J. E., 1870: *Catalogue of Monkeys, Lemurs, and Fruit-Eating Bats in the Collection of the British Museum*, viii + 137 p. Trustees of the British Museum (Natural History), London.
- Harada, Y., Ogawa, K., Mori, S., Kobayashi, S., Kubo, H. and Kiyosue, T., 1989: Variation of dentition in raccoon dogs (*Nyctereutes procyonoides viverrinus* T.) — Anomalies in number of the teeth—. *Japanese Journal of Oral Biology*, **31**: 257–264. (in Japanese with English abstract)
- Harada, Y., Ogawa, K., Mori, S., Kobayashi, S. and Nagamoto, S., 1992: Anomalous teeth of the raccoon dogs (*Nyctereutes procyonoides viverrinus* T.) — Shape, position and occlusion—. *Japanese Journal of Oral Biology*, **34**: 467–480. (in Japanese with English abstract)
- Kauhala, K., Viranta, S., Kishimoto, M., Helle, E. and Obara, I., 1998: Skull and tooth morphology of Finnish and Japanese raccoon dogs. *Annales Zoologici Fennici*, **35**: 1–16.
- Kusuhashi, N. and Okamoto, T., 2015: A nonparametric multimodality test—Silverman’s test—and its introduction into paleontology. *Fossils (The Palaeontological Society of Japan)*, **97**: 23–37. (in Japanese with English title)
- Machida, K. and Saito, T., 1986: Age structure and dental numerical anomalies of the raccoon dogs, *Nyctereutes procyonoides viverrinus* Temminck, in Chichibu District, Saitama Prefecture. *Bulletin of the Saitama Museum of Natural History*, **4**: 15–20. (in Japanese with English abstract)
- Silverman, B. W., 1981: Using kernel density estimates to investigate multimodality. *Journal of the Royal Statistical Society, Series B*, **43**: 97–99.
- Silverman, B. W., 1983: Some properties of a test for multimodality based on kernel density estimates. In, Kingman, J. F. C. and Reuter, G. E. H., eds., *Probability, Statistics and Analysis, London Mathematical Society Lecture Series*, **79**: 248–259. Cambridge University Press, London.
- Temminck, C. J., 1838: Over de kennis en de Verbreiding der Zoogdieren van Japan. *Tijdschrift Voor Natuurlijke Geschiedenis en Physiologie*, **5**: 273–293.
- Tsubamoto, T., 2014: Estimating body mass from the astragalus in mammals. *Acta Palaeontologica Polonica*, **59**: 259–265.
- Tsubamoto, T., 2015: Rare anomalous dental morphologies found in raccoon dog (*Nyctereutes procyonoides*) and their implication to dental morphology of fossil mammals. *Journal of the Geological Society of Japan*, **121**: 185–189.
- Tsubamoto, T., 2019a: Intraspecific variations of the astragalar and calcaneal sizes in living Japanese monkey (*Macaca fuscata*). *Memoirs of the Faculty of Science, Ehime University*, **22**: 1–17.
- Tsubamoto, T., 2019b: Relationship between the calcaneal size and body mass in primates and land mammals. *Anthropological Science*, **127**: 73–80.
- Tsubamoto, T., Egi, N., Takai, M., Thaung-Htike and Zin-Maung-Maung-Thein, 2016: Body mass estimation from the talus in primates and its application to the Pondaung fossil amphipithecid primates. *Historical Biology*, **28**: 27–34.
- Yamamoto, T., 1983: A comparative morphological study of tooth in raccoon dogs. *Journal of the Kyushu Dental Society*, **37**: 1–29. (in Japanese with English abstract)
- Yoshimura, K., 1983: A comparative anatomical study on the mandibulae of raccoon dogs. *Journal of the Kyushu Dental Society*, **37**: 663–679. (in Japanese with English abstract)

## Appendix

Appendix (Table A1 and Figures A1–A3) is available from <http://www.sci.ehime-u.ac.jp/wp/research/bulletin/>.